Food Chemistry 407 (2023) 135112

Contents lists available at ScienceDirect

Food Chemistry

journal homepage: www.elsevier.com/locate/foodchem

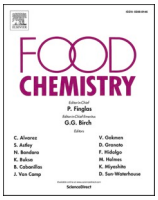

Linseed oil supplementation and *DGAT1* K232A polymorphism affect the triacylglycerol composition and crystallization of milk fat

N. Arita-Merino [a,b,1], S. Yener [a,1], H.J.F. van Valenberg [a], J. Dijkstra [d], S. van Gastelen [e], E. Scholten [b], D.A. Tzompa-Sosa [c,*]

[a] *Food Quality and Design Group, Wageningen University & Research, PO Box 17, 6700 AA Wageningen, the Netherlands*
[b] *Physics and Physical Chemistry of Foods, Wageningen University & Research, PO Box 17, 6700 AA Wageningen, the Netherlands*
[c] *Food Structure & Function Research Group, Department of Food Technology, Safety and Health, Faculty of Bioscience Engineering, Ghent University, Coupure Links 653, 9000B Ghent, Belgium*
[d] *Animal Nutrition Group, Wageningen University & Research, PO Box 338, 6700 AH Wageningen, the Netherlands*
[e] *Wageningen Livestock Research, Wageningen University & Research, PO Box 338, 6700 AH Wageningen, the Netherlands*

ARTICLE INFO

Keywords:
Unsaturated fat
Odd-chain
Fatty acid
Genetic
Diet
Dairy

ABSTRACT

We studied the effect of dietary linseed oil (LSO) supplementation and *DGAT1* K232A (*DGAT1*) polymorphism on the triacylglycerol composition and crystallization of bovine milk fat. LSO supplementation increased unsaturated triacylglycerols, notably in the C52–C54 carbon range, while reducing the saturated C29–C49 triacylglycerols. These changes were associated with an increase in the low-melting fraction and the crystal lamellar thickness, as well as a reduction in the medium and high-melting fractions and the formation of the most abundant crystal type at 20 °C (β'-2 polymorph). Furthermore, *DGAT1* KK was associated with higher levels of odd-chain saturated triacylglycerols than *DGAT1* AA, and it was also associated with an increase in the high-melting fraction and the endset melting temperature. An interaction between diet and *DGAT1* for the unsaturated C54 triacylglycerols accentuated the effects of LSO supplementation with *DGAT1* AA. These findings show that genetic polymorphism and cows' diet can have considerable effects on milk fat properties.

1. Introduction

Alternative feeding sources and genetic breeding have been frequently explored as possible strategies for achieving sustainability and productivity goals in dairy farming. However, farming practice modifications can alter the characteristics of milk, particularly milk fat (MF). Genetic, nutritional and environmental factors cause substantial variation in the triacylglycerol (TG) profile of MF and the associated fatty acid (FA) profiles (Jacobs et al., 2011; Palmquist, 2006; Soyeurt et al., 2007). As various TG molecules can crystallize into different structures (polymorphs) with varying properties, changes in the chemical composition of MF affect its physical properties and functionality (Lopez, 2018). Thus, to maintain MF functionality in dairy products (e.g. butter spreadability and cream whippability), the effect of farming practice changes on the chemical and physical properties of MF must be evaluated.

Van Gastelen et al. (2017) showed that linseed oil (LSO) supplementation and *DGAT1* K232A polymorphism significantly effect MF composition. *DGAT1* K232A polymorphism (*DGAT1*) is a polymorphism in the gene encoding for acyl CoA:diacylglycerol acyltransferase 1, a key enzyme in TG synthesis. Van Gastelen et al. (2017) reported a decrease in C6:0–C17:0 and an increase in both C18:0 and most unsaturated C_{18} fatty acids (FAs) upon LSO supplementation. Additionally, compared to *DGAT1* AA genotype, *DGAT1* KK was associated with higher C15:0, C16:0, C16:1 *cis*-9 and C14:1 *cis*-9, as well as a lower amount of several unsaturated C_{18} FAs. These changes in the FA profile aligned with those found by other studies utilizing LSO supplementation (Castro et al., 2019) and *DGAT1* (Lu et al., 2015).

Previous studies have shown that LSO supplementation affects the technological and physical properties of MF. For example, variations in the FA profile caused by linseed supplementation have been found to result in softer butter (Vanbergue et al., 2018) and cheese (Bocquel

* Corresponding author.
E-mail addresses: hein.vanvalenberg@wur.nl (H.J.F. van Valenberg), jan.dijkstra@wur.nl (J. Dijkstra), sanne.vangastelen@wur.nl (S. van Gastelen), elke.scholten@wur.nl (E. Scholten), daylan.tzompa@ugent.be (D.A. Tzompa-Sosa).
[1] Equal contribution.

https://doi.org/10.1016/j.foodchem.2022.135112
Received 6 July 2022; Received in revised form 25 November 2022; Accepted 25 November 2022
Available online 29 November 2022

et al., 2016). In MF, linseed supplementation has been shown to result in a lower solid fat content (SFC) at 5–30 °C (Smet et al., 2010), a higher proportion of the low-melting fraction (LMF), and changes in the formation of crystalline structures (Bugeat et al., 2015; Smet et al., 2010). While no studies have described the effect of *DGAT1* on the physical properties of MF, the effects of *DGAT1* on TG composition have been reported; compared to *DGAT1* AA, *DGAT1* KK has been associated with higher levels of TG groups with total carbon numbers C36 and C38 (Pacheco-Pappenheim et al., 2019; Tzompa-Sosa et al., 2016).

Both LSO supplementation and *DGAT1* can influence the composition, physical properties and, ultimately, functionality of MF. However, no studies have linked chemical composition changes (TAG, FA) with changes in MF physical properties. Determining this linkage could help control MF properties when new farming practices are adopted or tailor MF properties by selecting a specific diet or genetic variant. Hence, our aim was to investigate the effects of LSO supplementation and *DGAT1* on the TG composition and physical properties of MF. Specifically, we focused on the relationship between changes in TG composition and crystallization and the melting behavior of MF.

We hypothesized that the increase in long-chain unsaturated FAs upon LSO supplementation (van Gastelen et al., 2017) would increase the levels of high molecular weight (HMW) TGs (i.e. C50–C54), which would modify the formation of crystal structures. We expected that the increase in lamellar thickness previously associated with LSO supplementation (Bugeat et al., 2015) would increase the thickness of the crystal nanoplatelets. Regarding the lateral packing of the acyl chains, we hypothesized that the formation of β polymorph crystals would be enhanced by the HMW TGs, as was proposed by Tzompa-Sosa et al. (2016). Regarding the effect of *DGAT1*, we expected that the higher levels of C36 and C38 TGs previously reported with *DGAT1* KK compared to those with *DGAT1* AA (Pacheco-Pappenheim et al., 2019; Tzompa-Sosa et al., 2016) would increase the proportion of the medium melting fraction (MMF) in MF.

2. Material and methods

2.1. Experimental design and milk collection

Milk samples and MF content and FA composition data were obtained from the study by van Gastelen et al. (2017). Detailed information on the experimental design; individual cows; and feeding, housing and milking conditions can be found in their publication (van Gastelen et al., 2017). Briefly, the experiment followed a crossover design with two dietary treatments: a control diet (CON) and an LSO supplemented diet. Lactating Holstein-Friesian cows—12 with the *DGAT1* KK genotype and 12 with the *DGAT1* AA genotype—were blocked in pairs according to their *DGAT1* genotype, parity, lactation stage and milk production. Within each block, the cows were randomly assigned to a dietary treatment sequence utilizing a crossover design with two periods. The treatment periods lasted 17 days and comprised a 12-day adaptation period followed by a 5-day measurement period. During the 5-day measurement period, milk samples were collected twice daily in a tube containing sodium azide for preservation. They were then analyzed for MF content (ISO 14637; ISO-IDF, 2004). Additionally, representative milk samples were collected twice daily. Sodium azide was added to these samples for preservation, and they were then pooled per cow and period and stored at −40 °C pending analysis.

2.2. Milk fat samples

For compositional analyses, fat was extracted from the 48 individual milk samples to obtain 12 MF samples per treatment combination. To assess the physical properties, the milk samples were pooled per treatment, and the fat was extracted to produce four representative samples. For both the compositional and the physical analyses, MF was extracted following the method described by Tzompa-Sosa et al. (2014).

2.3. Triacylglycerol composition

Triacylglycerol composition was assessed with a combination of two complementary approaches: a quantification of TG groups based on total carbon numbers using GC-FID and qualitative profiling based on total carbon number and double bonds using MALDI-TOF-MS (Guyon et al., 2003; Tzompa-Sosa et al., 2016; Tzompa-Sosa & Arita-Merino, 2022). MALDI-TOF-MS provides a detailed fingerprint of MF TGs, but unlike GC-FID, it does not allow for absolute quantification of components, because MALDI-TOF-MS has different sensitivity to smaller and larger TGs (Fuchs et al., 2010).

The quantification of TG groups by GC-FID was performed according to ISO method 17678:2010(E) (IDF-ISO, 2010) using an UltiMetal CP7532 column (5 m × 0.53 mm × 0.17 μm f.t., Varian). This method allows 16 TG groups with total carbon numbers ranging from 24 to 54 (C24–C54) to be quantified. Each group consists of consecutive even- and odd-chain TGs (e.g. C40 corresponds to TGs with 40 and 41 total carbon numbers). The average TG compositions were expressed as mass fractions (g/100 g) of the total TG in MF.

The samples were prepared for TG profiling using MALDI-TOF-MS (Ultraflextreme, Bruker) as described by Picariello et al. (2007). They were then analyzed according to the procedure described by Tzompa-Sosa et al. (2018) using the auto-execute mode. The average spectra of each analysis comprised seven technical replicates. The mass spectrum of each replicate was the average of 1000 laser shots taken on 20 areas within the sample spot (50 shots per area). Masses with a signal-to-noise ratio higher than 6 were used for data processing. The relative abundance of a TG specie was calculated based on the sum of the intensities of all peaks. Each detected mass (±0.03 m/z) was assigned to a TG using a computationally generated database available in the LIPID MAPS® online tool (Fahy et al., 2007).

2.4. Thermal behavior

To study the dynamic and isothermal crystallization and melting profile of the four pooled MF samples, we used differential scanning calorimetry (DSC) (Discovery DSC25, TA Instruments). Aliquots of 10 ± 0.5 mg were weighed in hermetically sealed 40-μl aluminum pans. Prior to each analysis, the crystal memory was erased by maintaining the sample at 60 °C for 10 min. Dynamic crystallization was examined during cooling from 60 °C to −40 °C at a cooling rate of 5 °C/min, followed by an isothermal period of 5 min at −40 °C. Subsequently, the melting profiles were recorded while heating the sample to 60 °C at a heating rate of 5 °C/min. Using the crystallization thermograms, we determined the onset temperature of crystallization and the peak temperatures for the recorded crystallization events. Using the melting thermograms, we determined the endset melting temperature and calculated the melting enthalpy for three temperature regions. Enthalpy below 10 °C was assigned to LMF, from 10 to 20 °C to the MMF and above 20 °C to the high-melting fraction (HMF). We interpreted the contribution of a given fraction to the total melting enthalpy as an estimate of the amount of fat transitioning in the corresponding temperature range.

We studied isothermal crystallization at 20 °C for 1 h after the samples were cooled from 60 °C to 20 °C at a cooling rate of 10 °C/min. According to the number of peaks in the thermogram, we identified whether the crystallization occurred in one or more steps. After the isothermal period, we recorded the melting profiles while heating the samples from 20 to 60 °C at a heating rate of 5 °C/min. We considered the integrated melting enthalpy as an indication of the amount of fat that crystallized during the isothermal period.

2.5. Crystal nanostructure

To study the effect of *DGAT1* and LSO supplementation on MF crystallization, we examined the crystalline phases formed during

isothermal crystallization at 20 °C. Prior to analysis, the samples were kept at 60 °C for 10 min to erase the crystal memory. Then, the samples were cooled from 60 °C to 20 °C at a rate of 10 °C/min and were kept at that temperature for 1 h. Different X-ray techniques were used to examine the crystal characteristics of various lengths: wide-angle X-ray diffraction (WAXD) was used for the lateral packing of the acyl chains, small-angle X-ray diffraction (SAXD) for the lamellar thickness, and small-angle X-ray scattering (SAXS) for the crystallite thickness.

We obtained WAXD and SAXD patterns using a powder diffractometer (D8 ADVANCE, Bruker) with Cu radiation (kα wavelength, λ = 0.154 nm) equipped with a temperature chamber (TTK600, Anton Paar). We recorded time-resolved patterns using Bragg-Brentano geometry in 0.01° steps of 0.1 s in the small-angle region (2θ of 0.8–3°) and in 0.02° steps of 0.1 s in the wide-angle region (2θ of 15–26°).

The SAXS patterns were recorded using a laboratory-based SAXS (Xeuss 3.0 Compact Q-Xoom, Xenocs) with an Eiger 2 R 1 M detector and a Cu Kα radiation source (λ = 0.154 nm) with a Peltier stage and a capillary holder in transmission mode. MF was introduced in a borosilicate glass capillary (1.5 diameter, 0.01 mm wall thickness; WJM-Glas). Prior to the analysis, the samples were kept at 60 °C for 10 min to erase the crystal memory. Then, the samples were cooled from 60 to 20 °C at 20 °C/min. The SAXS patterns were recorded after 2 h at 20 °C under the following conditions: a sample-to-detector distance of 1080 mm, a 2θ range of 0.14–3.3° and an exposure time of 45 s, with 16 s between exposures.

The scattering angle 2θ was converted to reciprocal lattice spacing *q* or *d*-spacings according to Bragg's law. Based on the *d*-spacings of the WAXD and SAXD peaks, we identified crystalline phases with differing subcell and lamellar structures (polymorphs). Changes in the subcell structure were identified from the *d*-spacings in the WAXD patterns, according to the literature (Lopez, 2018). We further analyzed the WAXD patterns to quantify the polymorphs.

2.5.1. Quantification of crystalline phases

The crystalline phases were quantified following the method described by Arita-Merino et al. (2020). Briefly, to obtain the area contribution of each phase, we decomposed the WAXD patterns by fitting a Pearson VII function to each diffraction peak. Then, we converted the area contributions into mass fractions using phase-specific response factors. These factors were experimentally determined for a reference sample using SFC measurements by low resolution nuclear magnetic resonance (NMR) (Arita-Merino et al., 2022).

Changes in the longitudinal stacking of TGs, which corresponded to the lamellar thickness, were determined from the *d*-spacing of the first-order diffraction peaks L_{001} in the SAXD patterns. From the background-subtracted SAXS patterns, we also calculated the average crystallite size (ACS), which corresponded to the nanoplatelet thickness. The L_{001} peaks were fitted with a Pearson VII function. From the best fit through the experimental data points, we obtained the full width at half maximum (FWHM), which we then used to determine the ACS according to the Scherrer equation, as follows: ACS = $K\lambda$/FWHM. As is common in fat studies, a shape factor *K* of 0.9 was used for simplicity (Acevedo & Marangoni, 2015). All calculations were completed using R programming language.

2.6. Data analysis

We assessed the individual and combined effects of LSO supplementation and *DGAT1* on the TG composition of MF with a linear mixed model using the Proc Mixed procedure in SAS/STAT statistical software version 9.4 (SAS Institute Inc). This model was based on that of van Gastelen et al. (2017), which included treatments (diet and *DGAT1*), their interaction, diet sequence, and period (e.g. LSO supplementation in period 1 and CON in period 2). Block was included as a random factor in the model, while cows were considered subjects within diet × *DGAT1*. To account for the differences in fat content reported by van Gastelen et al. (2017), MF content was introduced as a covariable in the model. The Tukey-Kramer method was used to make pairwise comparisons of the means of the TG compositions under the two main factors: diet and *DGAT1*. A *p*-value $\leq$ 0.05 was used throughout the study to highlight significant differences. As the physical properties were determined for the samples pooled per treatment (n = 4), we focused on sizable differences consistent for a given diet or *DGAT1* variant. Therefore, we only considered differences larger than 0.5 °C for peak, onset and endset temperatures; 0.1 nm for lamellar thickness; 0.1 nm for ACS; and 10 % for all other parameters studied.

3. Results and discussion

3.1. Milk fat composition

To study the effect of LSO supplementation and *DGAT1* on the TG composition of MF, we combined two analytical techniques: GC-FID and MALDI-TOF-MS. We used GC-FID to quantify 16 TG groups (Table 1), and MALDI-TOF-MS (Table 2) to create a fingerprint of MF TGs, through which we identified 71 TGs with various carbon atoms and double bonds.

3.1.1. Effect of LSO supplementation on TG composition

Diet notably modified the composition of MF, exerting a significant effect on all TG groups (except C50; see Table 1) and on 59 TGs (Table 2). Compared to CON, LSO supplementation increased the content of TG groups C40, C52 and C54 while lowering the levels of the remaining TG groups. We attributed the increased content of the C40, C52 and C54 groups to increased levels of unsaturated TG species, specifically TG species TG 40:3, TG 40:2, TG 40:1, TG 52:1, TG 52:2, and TG 54:3. Regarding C54 and its unsaturated TGs we observed a significant interaction between diet and *DGAT1* (Subsection 3.1.3). Although LSO supplementation increased the levels of all polyunsaturated TGs, from TG 36:2–TG 54:5, this increase was not reflected in groups with lower molecular weight, which are predominantly composed of saturated and monounsaturated species. The decreased contents of TG groups C24–C38 and C42–C48 after LSO supplementation can be explained by the decreased levels of saturated TGs, including all species from TG 29:0–TG 49:0 (with the exception of TG 42:0). The reduction in TG groups C44–C48 after LSO supplementation also coincided with a reduction in monounsaturated TGs from TG 44:1–TG 50:1.

Our findings concerning the effect of LSO supplementation on TG composition aligned with the effect on FA composition reported by van Gastelen et al. (2017). They found higher concentrations of C_{18} FAs, which coincided with higher HMW TGs in our study. Van Gastelen et al. (2017) related this increased C_{18} proportion to the high C18:3 *cis*-9,12,15 intake with LSO and the subsequent high level of biohydrogenation intermediates (e.g. C18:1 *trans*-11) and end products (C18:0) in MF. Our results showed that excess C_{18} FAs were largely incorporated into more unsaturated TGs in groups C40, C52 and C54. The lower levels of saturated and smaller TGs after LSO supplementation also coincided with the lower concentrations of *de novo* synthesized FAs (C16:0, short- and medium-chain FAs) previously reported by van Gastelen et al. (2017). This decrease in the saturated *de novo* FAs (C6:0–C16:0) explained the reduction in saturated TG 29:0–TG 49:0 we observed. The decrease in saturated FAs in both C10:0–C16:0 and C14:1 *cis*-9 and C16:1 *cis*-9 (van Gastelen et al., 2017) explained the lower levels of monounsaturated TGs from TG 44:1–TG 50:1, as these FAs are important constituents of monounsaturated TGs in that size range (Gresti et al., 1993). To the extent of our knowledge, our study is the first to report the effect of LSO supplementation on MF TG composition.

The effect of LSO supplementation on MF TG composition that we observed agreed with other related studies on the effect of higher intake of C_{18} fatty acids from sources other than linseed. For example, MF obtained after supplementing the cows' diet with canola oil showed higher concentrations of TG groups C50–C54 (DePeters et al., 2001).

Table 1
GC-FID triacylglycerol (TG) composition (g/100 g TG) of milk fat from cows with two *DGAT1* variants (AA or KK), fed a diet supplemented with linseed oil (LSO) or a control diet (CON).

TG group	Treatment					*p*-value		
	CON *DGAT1* AA	CON *DGAT1* KK	LSO *DGAT1* AA	LSO *DGAT1* KK	SEM	Diet	*DGAT1*	Diet × *DGAT1*
C24	0.06	0.09	0.04	0.04	0.01	**0.012**	0.326	0.308
C26	0.20	0.19	0.17	0.17	0.01	**0.004**	0.654	0.371
C28	0.55	0.49	0.44	0.44	0.01	**0.003**	0.986	0.299
C30	1.14	1.06	0.85	0.85	0.03	**< 0.001**	0.715	0.373
C32	2.55	2.41	1.73	1.77	0.07	**<0.001**	0.604	0.359
C34	5.98	5.81	3.77	4.00	0.18	**<0.001**	0.760	0.254
C36	10.46	10.83	7.21	7.97	0.27	**<0.001**	**0.040**	0.496
C38	11.52	11.78	9.94	10.90	0.16	**<0.001**	**0.010**	0.158
C40	9.30	9.04	10.56	10.52	0.15	**<0.001**	0.643	0.672
C42	7.38	7.31	6.19	6.41	0.12	**<0.001**	0.174	0.344
C44	7.29	7.37	5.10	5.47	0.18	**<0.001**	0.309	0.332
C46	8.18	8.41	6.07	6.50	0.18	**<0.001**	0.850	0.507
C48	9.96	10.23	8.03	8.58	0.16	**<0.001**	0.281	0.418
C50	11.46	11.70	12.08	12.13	0.15	0.126	0.777	0.760
C52	9.13	8.79	13.70	12.96	0.42	**<0.001**	0.533	0.701
C54	4.61[c]	4.19[c]	13.93[a]	11.09[b]	0.66	**<0.001**	0.120	**0.011**

SEM: standard error of measurement. Numbers in bold correspond to *p*-values below the 0.05 threshold. Superscripts indicate differences (p-values < 0.05) based on Tukey-Kramer pairwise comparisons.

Similarly, the levels of C50–C54 in MF increase in summer, when cows have a higher C18:3 *cis*-9,12,15 intake from fresh grass (Pacheco-Pappenheim et al., 2021). As in the present study, the increase in HMW TGs in summer is associated with higher levels of unsaturated TGs (Pacheco-Pappenheim et al., 2021). Pacheco-Pappenheim et al. (2022) recently reported that high-fat diets containing hydrogenated palm FAs (C18:0 and C16:0) were associated with an increase in C50–C52. However, the intake of saturated long-chain FAs was associated with higher levels of unsaturated HMW TGs and saturated TG 50:0–TG 54:0, whereas the only saturated specie that increased was TG 52:0 in the cases of LSO supplementation (Table 2) and MF in summer (Pacheco-Pappenheim et al., 2021).

3.1.2. Effect of DGAT1 on TG composition

The *DGAT1* AA variant often dominates over AK and KK variants in dairy herds (Kaupe et al., 2004). *DGAT1* KK can be found in a varying percentage, for example: 1 % in Swedish Red breed (Näslund et al., 2008), 3 % in Swedish Holstein breed (Näslund et al., 2008) and 16 % of cows sampled from 398 commercial herds from the Netherlands (Schennink et al., 2008). The dominance of *DGAT1* AA in dairy cattle could be explained by selection prioritizing milk yield (Kaupe et al., 2004), which is associated with *DGAT1* AA. Still the frequency of the *DGAT1* K allele in herds of different dairy breeds varies widely (2–69 %) (Kaupe et al., 2004). Thus, *DGAT1* can be important for effective breeding, targeting specific properties in milk fat.

Compared to LSO supplementation, *DGAT1* showed a less pronounced effect on TG composition. TG groups C36 and C38 were higher for *DGAT1* KK than for *DGAT1* AA (Table 1), but the differences were modest (<1 g/100 g). The results also indicated that C54 was lower for *DGAT1* KK, and although this difference was not significant, we did observe a significant diet × *DGAT1* effect (Subsection 3.1.3). The MALDI-TOF-MS results showed that the odd-chain saturated TG 31:0–TG 41:0 and the monounsaturated TG 37:1 and TG 41:1 were higher for *DGAT1* KK than for *DGAT1* AA (Table 2). Thus, the higher levels of TG groups C36 and C38 with *DGAT1* KK may have resulted from incorporating more saturated and monounsaturated odd-chain TGs (i.e. TG 37:0, TG 39:0 and TG 37:1) in that total carbon number range. Similar associations between *DGAT1* KK and higher levels of odd-chain TGs have been reported previously (Pacheco-Pappenheim et al., 2019; Tzompa-Sosa et al., 2016). *DGAT1* KK has been associated with higher proportions of C15:0, C16:0, C14:1 *cis*-9 and C16:1 *cis*-9 and lower proportions of several C_{18} unsaturated fatty acids (UFAs) (van Gastelen et al., 2017). Therefore, the increase in monounsaturated and odd-chain TGs for *DGAT1* KK could result from the higher abundance of C14:1 *cis*-9 and C16:1 *cis*-9 and C15:0, respectively.

3.1.3. Interaction of DGAT1 and LSO supplementation

Besides the individual effects of diet and *DGAT1* on TG composition, a significant interaction between diet and *DGAT1* indicated that the increase in C54 with LSO supplementation was more pronounced with *DGAT1* AA than with *DGAT1* KK (Table 1). The MALDI-TOF-MS results confirmed this interaction (Table 2). For visualization, Fig. 1 shows the results for different unsaturated TGs corresponding to the C54 group, allowing comparison of the effect of *DGAT1* for the two diets. LSO supplementation resulted in increased levels of TG 54:4, TG 54:3, TG 54:2 and TG 54:1 for both *DGAT1* AA and *DGAT1* KK. The increase was more pronounced for *DGAT1* AA than for *DGAT1* KK. These HMW unsaturated TGs likely contain C_{18} FAs (Liu et al., 2020). However, van Gastelen et al. (2017) found diet × *DGAT1* interactions for C14:0 and C15:0 only. LSO supplementation and *DGAT1* AA result in increased proportions of several C_{18} FAs in MF compared with CON and *DGAT1* KK, respectively (van Gastelen et al., 2017). Thus, the increased levels of these FAs may increase the formation of unsaturated HMW TGs beyond the separate effects of LSO and *DGAT1* AA (i.e. a synergistic effect). This synergistic effect of LSO and *DGAT1* AA on the levels of HMW unsaturated TGs aligns with other reported diet × *DGAT1* interactions. For example, higher levels of C52 in MF have been associated with *DGAT1* AA when the C18:3 *cis*-9,12,15 intake increases in summer, whereas the change associated with *DGAT1* AA in winter is not significant (Pacheco-Pappenheim et al., 2019).

We also found an interaction effect for TG 44:0. For both *DGAT1* AA and *DGAT1* KK, LSO supplementation compared with CON resulted in a decrease in TG 44:0, but this effect was more pronounced for *DGAT1* AA (-36 %) than for *DGAT1* KK (-28 %; Table 2). A similar diet × *DGAT1* effect has been reported for C42; *DGAT1* KK was associated with lower C42 levels in winter, when cows have a lower intake of C18:3 *cis*-9,12,15, and higher levels in summer (Pacheco-Pappenheim et al., 2019).

Overall, diet had a large effect on TG composition, whereas the effect of *DGAT1* appeared to be moderate but highly specific. Compared with CON, LSO supplementation increased the levels of unsaturated TGs, most notably in groups C40 and C52. The main *DGAT1* effect corresponded to higher levels of odd-chain saturated TGs (TG 31:0–TG 41:0) with *DGAT1* KK compared to *DGAT1* AA. Additionally, we identified diet × *DGAT1* interactions for the unsaturated TGs in the C54 group and TG 44:0. We expected these changes in TG composition to influence the

Table 2
MALDI-TOF-MS triacylglycerol (TG) profile (relative intensity, %) of milk fat from cows with two *DGAT1* variants (AA or KK), fed a diet supplemented with linseed oil (LSO) or a control diet (CON).

TG	Treatment					*p*-value		
	CON *DGAT1* AA	CON *DGAT1* KK	LSO *DGAT1* AA	LSO *DGAT1* KK	SEM	Diet	*DGAT1*	Diet × *DGAT1*
TG 26:0	0.31	0.29	0.27	0.27	0.01	0.451	1.000	0.313
TG 28:0	0.74	0.67	0.64	0.63	0.03	0.312	0.592	0.374
TG 29:0	0.16	0.17	0.14	0.16	0.00	**0.001**	0.254	0.791
TG 30:0	1.35	1.18	1.04	1.05	0.10	**0.008**	0.817	0.459
TG 31:0	0.28	0.31	0.21	0.24	0.00	**<0.001**	**0.048**	0.623
TG 32:1	0.56	0.49	0.63	0.60	0.02	0.319	0.763	0.690
TG 32:0	2.21	2.02	1.64	1.41	0.08	**0.001**	**0.022**	0.669
TG 33:2	0.18	0.27	0.12	0.18	0.01	n.d.	n.d.	n.d.
TG 33:1	0.16	0.16	0.20	0.21	0.00	**<0.001**	0.169	0.549
TG 33:0	0.36	0.41	0.31	0.34	0.00	**<0.001**	**0.016**	0.242
TG 34:1	0.97	0.89	0.73	0.56	0.10	**0.003**	0.505	0.468
TG 34:0	4.54	4.42	2.84	3.05	0.24	**<0.001**	0.794	0.102
TG 35:0	0.72	0.92	0.53	0.62	0.02	**<0.001**	**0.001**	0.054
TG 36:2	0.34	0.32	0.47	0.46	0.00	**<0.001**	0.077	0.859
TG 36:1	2.31	2.28	2.39	2.36	0.04	0.354	0.836	0.996
TG 36:0	6.17	6.56	3.92	4.48	0.46	**<0.001**	0.540	0.428
TG 37:1	0.46	0.49	0.51	0.53	0.00	0.181	**0.044**	0.471
TG 37:0	0.96	1.10	0.71	0.83	0.01	**<0.001**	**0.005**	0.464
TG 38:2	0.86	0.84	1.19	1.20	0.02	**<0.001**	0.354	0.553
TG 38:1	4.21	4.28	4.34	4.49	0.14	0.066	0.609	0.574
TG 38:0	4.79	5.11	3.33	3.84	0.27	**<0.001**	0.623	0.215
TG 39:1	0.56	0.58	0.67	0.70	0.01	**<0.001**	0.062	0.679
TG 39:0	0.85	0.93	0.69	0.82	0.02	**<0.001**	**0.007**	0.655
TG 40:3	0.33	0.29	0.80	0.73	0.02	**<0.001**	0.682	0.275
TG 40:2	1.35	1.21	2.70	2.42	0.08	**<0.001**	0.782	0.282
TG 40:1	3.10	3.11	3.63	3.64	0.07	**<0.001**	0.795	0.998
TG 40:0	3.21	3.36	2.26	2.51	0.14	**<0.001**	0.938	0.248
TG 41:2	0.50	0.17	0.34	0.33	0.26	**0.001**	0.604	0.664
TG 41:1	0.45	0.46	0.57	0.61	0.01	**<0.001**	**0.048**	0.624
TG 41:0	0.67	0.73	0.55	0.65	0.01	**<0.001**	**0.020**	0.761
TG 42:2	0.78	0.72	1.24	1.15	0.01	**<0.001**	0.137	0.323
TG 42:1	2.15	2.17	2.06	2.08	0.05	0.563	0.364	0.893
TG 42:0	2.56	2.57	1.51	1.67	0.09	**<0.001**	0.526	0.154
TG 43:1	0.40	0.42	0.40	0.43	0.01	0.863	0.203	0.926
TG 43:0	0.53	0.57	0.40	0.47	0.01	**<0.001**	0.073	0.594
TG 44:2	0.69	0.69	0.78	0.77	0.01	**<0.001**	0.960	0.410
TG 44:1	2.17	2.21	1.69	1.78	0.05	**<0.001**	0.491	0.549
TG 44:0	1.76[a]	1.69[a]	1.12[b]	1.21[b]	0.03	**<0.001**	0.231	**0.031**
TG 45:1	0.40	0.43	0.36	0.39	0.00	**0.005**	0.213	0.933
TG 45:0	0.49	0.50	0.36	0.42	0.00	**<0.001**	0.184	0.154
TG 46:2	0.85	0.83	1.06	1.00	0.01	**<0.001**	0.350	0.255
TG 46:1	2.23	2.29	1.83	1.86	0.04	**<0.001**	0.367	0.919
TG 46:0	1.30	1.22	0.88	0.92	0.01	**<0.001**	0.159	0.066
TG 47:1	0.50	0.53	0.47	0.50	0.00	**0.027**	0.198	0.880
TG 47:0	0.48	0.48	0.36	0.41	0.00	**<0.001**	0.193	0.233
TG 48:3	0.26	0.26	0.37	0.36	0.00	**<0.001**	0.691	0.418
TG 48:2	1.11	1.13	1.24	1.21	0.03	**0.006**	0.894	0.689
TG 48:1	2.94	2.92	2.45	2.45	0.06	**<0.001**	0.159	0.609
TG 48:0	1.01	0.95	0.79	0.80	0.01	**<0.001**	0.324	0.168
TG 49:1	0.74	0.78	0.67	0.69	0.01	**<0.001**	0.391	0.532
TG 49:0	0.52	0.50	0.41	0.43	0.01	**<0.001**	0.395	0.199
TG 50:3	0.48	0.46	0.83	0.75	0.02	**<0.001**	0.823	0.259
TG 50:2	1.82	1.78	2.39	2.17	0.10	**<0.001**	0.153	0.131
TG 50:1	3.25	3.37	2.93	2.89	0.11	**0.001**	0.431	0.193
TG 50:0	0.74	0.67	0.72	0.71	0.01	0.450	0.190	0.307
TG 51:2	0.45	0.44	0.65	0.61	0.02	**<0.001**	0.900	0.239
TG 51:1	0.72	0.72	0.84	0.80	0.01	**0.015**	0.846	0.378
TG 51:0	0.49	0.46	0.47	0.44	0.01	0.312	0.761	0.675
TG 52:4	0.26	0.25	0.46	0.43	0.01	**<0.001**	0.831	0.755
TG 52:3	0.80	0.76	1.44	1.27	0.08	**<0.001**	0.419	0.234
TG 52:2	2.49	2.38	3.49	3.18	0.39	**<0.001**	0.453	0.385
TG 52:1	1.71	1.64	2.35	2.16	0.10	**<0.001**	0.249	0.454
TG 52:0	0.34	0.31	0.40	0.40	0.00	**<0.001**	0.505	0.517
TG 53:2	0.42	0.40	0.70	0.64	0.03	**<0.001**	0.912	0.448
TG 53:1	0.54	0.51	0.77	0.73	0.02	**<0.001**	0.971	0.860
TG 54:5	0.18	0.15	0.40	0.32	0.01	**<0.001**	0.948	0.165
TG 54:4	0.30[c]	0.25[c]	1.06[a]	0.79[b]	0.03	**<0.001**	0.258	**0.005**
TG 54:3	0.77[c]	0.61[c]	2.42[a]	1.82[b]	0.17	**<0.001**	0.118	**0.010**
TG 54:2	0.75[c]	0.61[c]	2.29[a]	1.78[b]	0.10	**<0.001**	0.088	**0.006**
TG 54:1	0.41[c]	0.35[c]	1.10[a]	0.88[b]	0.02	**<0.001**	0.094	**0.015**
TG 54:0	0.15	0.11	0.17	0.17	0.00	n.d.	n.d.	n.d.

SEM: standard error of measurement. n.d. *p*-values were not calculated due to low number of observations for these TGs. Numbers in bold correspond to *p*-values below the 0.05 threshold. Superscripts indicate differences (*p*-values < 0.05) based on Tukey-Kramer pairwise comparisons.

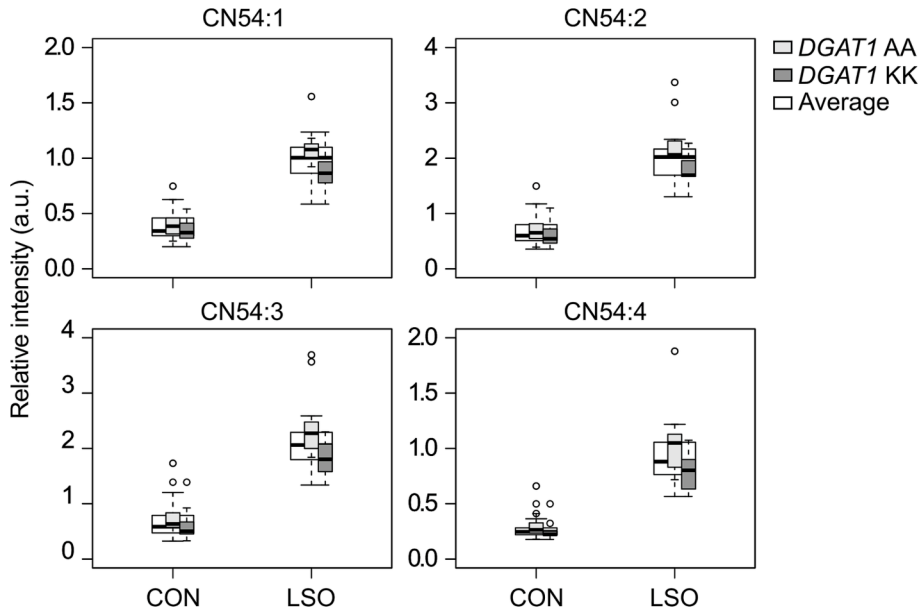

Fig. 1. Relative intensities (a.u.) of triacylglycerols TG 54:1, TG 54:2, TG 54:3, and TG 54:4 of milk fat from cows of two *DGAT1* variants (AA or KK), fed a linseed oil supplemented diet (LSO) or a control diet (CON).

physical properties of MF.

3.2. Effect of DGAT1 and LSO supplementation on MF crystallization

To investigate whether the changes in TG composition associated with LSO supplementation and *DGAT1* affected the physical properties of MF, we studied the crystallization behavior. In this section, our objective was to identify sizeable differences that could affect the functionality of MF as a food ingredient, rather than determine whether the effect of a treatment was statistically significant. Analyzing the 48 samples using X-ray techniques would have been prohibitive, therefore, we analyzed four representative samples obtained blending the 12 samples per treatment. Although we observed several changes consistent to a given diet or *DGAT1* variant, we focused on sizeable changes only due to the limited number of samples. Minor components present in MF (e.g. partial glycerides and fatty acids) can affect the kinetics of

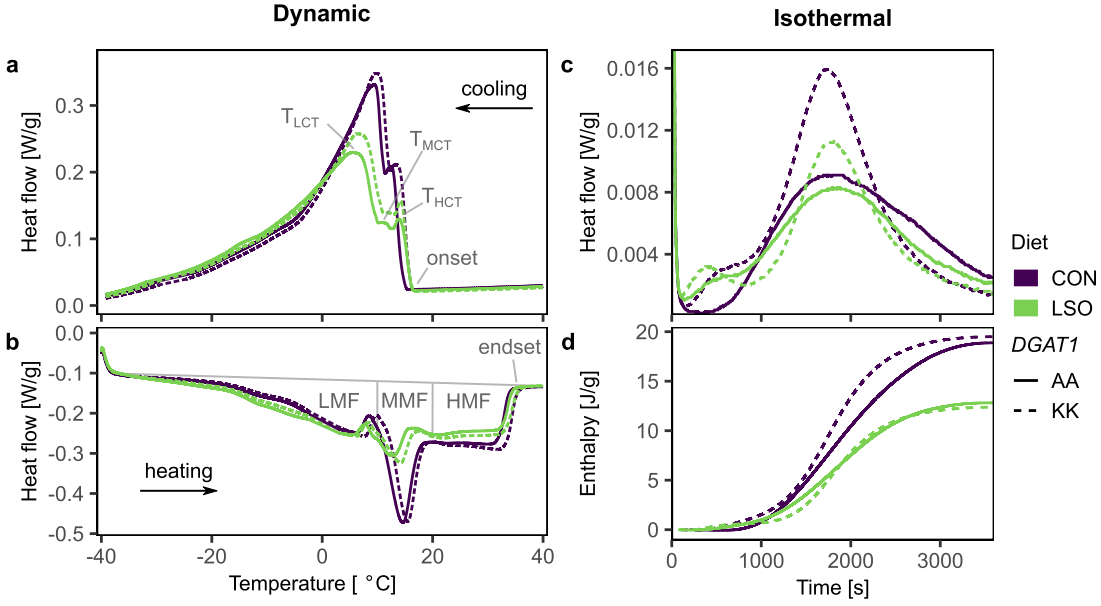

Fig. 2. Thermograms of milk fat from cows of two *DGAT1* variants (AA or KK), fed a linseed oil (LSO) supplemented diet or a control diet (CON). Dynamic crystallization (a) and melting curves (b) recorded at 5 °C/min. The peak temperature for the high, medium and low crystallization temperature TGs (T_{HCT}, T_{MCT} and T_{LCT}, respectively) are indicated in (a). Grey marks illustrate the parameters determined from the curves, taking LSO-AA as an example. The melting enthalpy for the low, medium and high melting fractions (LMF, MMF and HMF, respectively) are indicated in (b). Isothermal crystallization curve (c) and corresponding evolution of the enthalpy of crystallization (d) recorded at 20 °C for 1 h.

crystallization, however, the microstructure, mechanical properties, dropping point and solid fat content remain unchanged (Wright & Marangoni, 2003; Wright et al., 2000a). While possible changes in the non-TG fraction (~2%) might influence the physical properties, here, we focus on the main components. The notable changes in TG profile we report here are expected to be the determinant factor driving changes in MF crystallization.

3.2.1. Crystallization and melting profiles

Using DSC, we obtained dynamic crystallization and melting curves for the samples (Fig. 2a and b) to determine parameters that we expected to be affected by the compositional changes in MF. These parameters are illustrated in Fig. 2a and b, and their values are included in Table 3.

As is typical for MF, we recorded two main exothermic peaks corresponding to two crystallization events in the four samples during cooling (Fig. 2a). These peaks have been attributed to the crystallization of two groups of TGs with high crystallization temperature (HCT) and low crystallization temperature (LCT), each forming a different structure (α-2 and α-3 polymorphs, respectively; Bugeat et al., 2015; Lopez, 2018). Changes in the peak temperatures for HCT (T_{HCT}) and LCT (T_{LCT}) TGs can thus be associated with the characteristics of the main TGs in those two groups. During heating (Fig. 2b), we observed three melting regions commonly identified in MF (Lopez, 2018): the LMF, MMF and HMF. As explained in Section 2.4, we interpreted a change in enthalpy for the different melting fractions as a change in their relative abundance.

While the four samples displayed the general features characterizing MF crystallization and melting profiles, we observed variations related to the compositional changes among the samples associated with diet and *DGAT1*. Most of these differences could be explained by the changes in TGs with different unsaturation levels and molecular weight, as the melting temperature of TGs is higher for saturated versus unsaturated species and for larger versus smaller molecules.

During crystallization, the LSO supplementation samples displayed slightly higher (0.5–0.8 °C increase) T_{HCT} and considerably lower (3.4–3.9 °C decrease) T_{LCT} values. Fig. 2a clearly shows that the increase in T_{HCT} did not correspond to a peak shift but rather a decline in the heat flow at higher temperatures. Therefore, both the higher T_{HCT} and lower T_{LCT} for the LSO supplementation samples could be explained by the lower levels of saturated TGs. Furthermore, the lower levels of TGs with higher molecular weight (e.g. TG 47:0, TG 48:0 and TG 49:0) may have been responsible for the decline of the HCT peak at higher temperatures, while the decrease in TGs in groups C36 and C42–C46 may have been responsible for the higher T_{LCT}. The LSO supplementation samples also displayed an additional intermediate crystallization peak at ~11 °C. In congruency with the classification used for the other two peaks (Lopez, 2018), we assigned the intermediate peak to a group of medium crystallization temperature (MCT) TGs (Fig. 2a). The occurrence of this additional MCT peak with LSO supplementation aligned with the results of Bugeat et al. (2015), who reported an additional crystallization peak at ~10 °C in their study of MF enriched with UFAs through LSO supplementation. They used XRD and DSC simultaneously to study the crystallization process and were able to associate this additional peak with the formation of a second α-2 phase with lower (~4.1 nm) lamellar thickness than that formed by the HCT TGs (~4.8 nm). LSO supplementation could increase the concentration of MCT TGs; however, as lamellar thickness increases with the size of its composing molecules, the thinner α-2 lamellae were unlikely formed by the higher levels of HMW TGs. Alternatively, the shift of the LCT peak to a lower temperature, combined with the decay of the HCT peak at a higher temperature, may have allowed us to observe a separate peak when the MCT TGs crystallized. This explanation aligns with the previous observation of a second α-2 phase with thinner lamellae in the absence of an additional peak at intermediate temperatures (Lopez et al., 2005).

Diet also affected the melting profiles. Compared to the CON samples, the abundance of LMF was ~12 % higher, the MMF was ~9 % lower, and the HMF fraction was ~4 % lower in the LSO supplementation samples. The increase in unsaturated TGs for LSO supplementation explained the higher LMF values, whereas the decrease in saturated TGs explained the lower MMF and HMF values. The increase in unsaturated TGs and the corresponding increase in LMF are likely to be responsible for major changes in MF crystallization. Low-melting-point TGs dissolve TGs with higher melting point, but their effect can go beyond simple dilution and solubilization. Wright et al. (2000b) showed that LMF, canola oil, hexane and ethyl acetate act as solvents for MMF and HMF; but unlike the other solvents, LMF forms complexes with the other two fractions, possibly due to molecular complementarity (Wright et al., 2000b). An enhanced formation of complexes in the LSO supplementation samples could explain the additional crystallization event we observed in the thermograms (T_{MCT} in Fig. 2a); further research is needed to test this hypothesis.

LSO supplementation affected the levels of TG groups in nearly the entire MF melting range. Nevertheless, the crystallization onset and the

Table 3
Parameters that characterize the crystallization and melting behavior of milk fat from cows of two *DGAT1* K232A variants (AA or KK), fed a linseed oil supplemented diet (LSO) or a control diet (CON).

Conditions	Technique	Parameter	CON *DGAT1* AA	CON *DGAT1* KK	LSO *DGAT1* AA	LSO *DGAT1* KK
Dynamic crystallization and melting	DSC	Crystallization onset [°C]	14.1	15.5	15.3	15.5
		T_{HCT} [°C]	12.4	13.4	13.9	14.2
		T_{MCT} [°C]	Not present	Not present	11.3	11.7
		T_{LCT} [°C]	9.4	9.8	5.5	6.4
		LMF [%]	36	35	50	45
		MMF [%]	34	31	23	25
		HMF [%]	30	34	27	30
		Melting endset [°C]	33.9	35.2	34.4	35.4
Isothermal crystallization at 20 °C for 1 h	DSC	Crystallization steps	1	2	2	2
		Total melting enthalpy [J/g]	26	30	23	25
	WAXD and SAXD	Max α-2 formed [%]	0	2	1	2
		Max β'-2 formed [%]	16	17	10	14
		Max β-2 formed [%]	1	1	1	2
		Final calculated SFC [%]	17	18	11	16
	SAXS	Final lamellar thickness [nm]	4.08	4.07	4.24	4.22
		Final ACS [nm]	56	57	52	57

DSC: differential scanning calorimetry. WAXD: wide angle X-ray diffraction. SAXD: small angle X-ray diffraction. SAXS: small angle X-ray scattering. T_{HCT}, T_{MCT}, and T_{LCT} correspond to the peak temperature for the high, medium, and low crystallization temperature triacyclglycerols, respectively. LMF, MMF, and HMF correspond to the melting enthalpy fraction for the low, medium, and high melting fractions, respectively. Solid fat content (SFC) calculated as the sum of the amount of β' and β polymorphs after 1 h at 20 °C. The average crystallite thickness (ACS) corresponds to the thickness of the crystal nanoplatelets.

melting endset for the LSO supplementation samples were not particularly different, which aligned with the findings of Bugeat et al. (2015). The TGs that initiate crystallization and those that melt at the highest temperature likely correspond to the same group, which was not affected by LSO supplementation to the extent of producing further changes in the crystallization and melting profiles.

Analogous to the compositional changes, the differences in crystallization and melting profiles associated with *DGAT1* were specific and less pronounced than those associated with LSO supplementation (Table 3). During cooling, compared to their *DGAT1* AA counterparts, the *DGAT1* KK samples consistently displayed higher (+0.3 to +1 °C) T_{HCT}, T_{MCT} and T_{LCT}. However, these differences were miniscule, and a larger sample set is necessary to confirm the observed trend. Only two differences in the melting profiles could be attributed solely to *DGAT1* (Fig. 2b). Based on the increments in C36 and C38 previously reported for *DGAT1* KK (Pacheco-Pappenheim et al., 2019; Tzompa-Sosa et al., 2016), we expected an increment in MMF. Instead, the *DGAT1* KK samples displayed slightly higher (3–4 %) HMF values compared to the

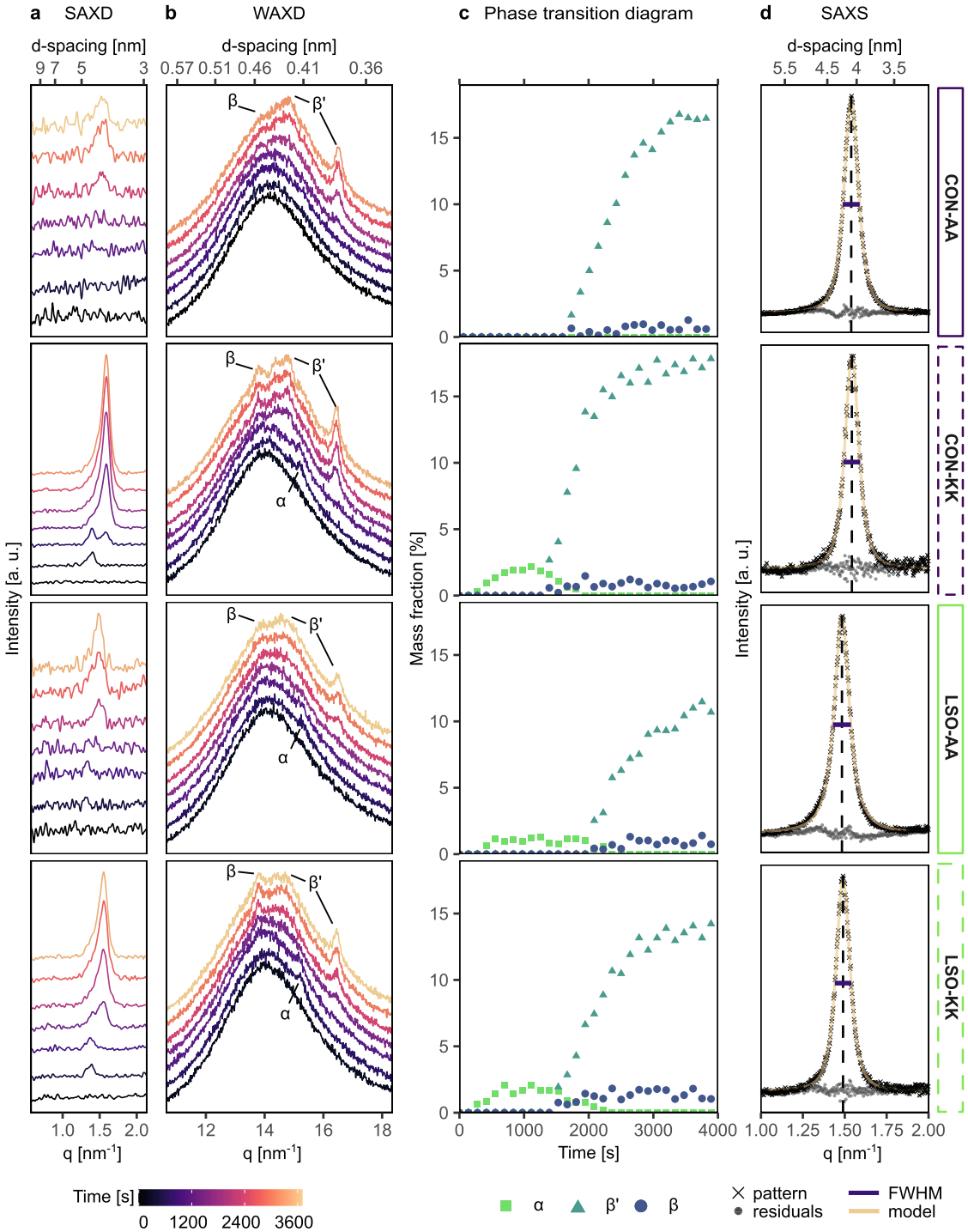

Fig. 3. Crystalline structures formed at 20 °C in milk fat from cows of two *DGAT1* variants (AA or KK), fed a linseed oil (LSO) supplemented diet or a control diet (CON). From left to right, representative time-resolved SAXD (a) and WAXD patterns (b), the corresponding phase transition diagrams (c), and the analysis of the SAXS patterns recorded after 1 h of crystallization (d).

DGAT1 AA samples. This could be explained by the higher levels of odd-chain saturated TGs with *DGAT1* KK. Additionally, whereas diet did not show a clear effect on the melting endset, the *DGAT1* KK samples displayed higher endset values (1–1.3 °C higher) than the *DGAT1* AA samples. This showed that *DGAT1* influences the synthesis of the TGs that melt last. Therefore, we expected saturated species with the highest molecular weight (e.g. TG 54:0) to be higher in the *DGAT1* KK MFs, but this was not the case. As miscibility also plays a role in a multicomponent system like MF, some of the odd-chain saturated TGs that are more abundant in *DGAT1* KK MFs may have melted at higher temperatures than other saturated species with higher molecular weight.

Compositional changes due to the combined effect of diet and *DGAT1* were also reflected in the crystallization and melting profiles. For LSO samples from the *DGAT1* AA genotype, the LMF was 5 % higher than that of the LSO samples from the *DGAT1* KK genotype, whereas we found no substantial difference between the two *DGAT1* varieties with the CON diet. This finding aligned with the larger increase in unsaturated C54 TGs for *DGAT1* AA than for *DGAT1* KK with LSO supplementation compared to CON (Table 2).

3.2.2. Isothermal crystallization studied by DSC

As we observed differences in the crystallization and melting profiles, we investigated whether the crystallization process would differ under isothermal conditions. We recorded crystallization curves for 1 h at 20 °C (Fig. 2c) and calculated the crystallization enthalpy by integrating the heat flow over time (Fig. 2d). To estimate the amount of crystalline matter formed, we measured the melting enthalpy after the crystallization period (Table 3). The melting enthalpy was lower for the LSO supplementation samples (23–25 J/g) compared to that of the CON samples (26–30 J/g). This indicated that less fat crystallized at 20 °C with LSO supplementation, likely due to the lower levels of saturated TGs. Not only did the extent of crystallization show differences, but also the way in which it took place. We observed two exothermic peaks for all samples, except for the CON and *DGAT1* AA sample, for which we observed only one peak (Fig. 2c). Therefore, this sample crystallized in one step, whereas the other three samples crystallized in two steps. As the number of steps in a crystallization process is associated with structural transitions (Arita-Merino et al., 2022), we investigated possible changes in the MF nanostructure.

3.2.3. Changes in the nanostructure during isothermal crystallization

We used various X-ray techniques to study the structural changes associated with the different crystallization processes identified by DSC. The SAXD and WAXD patterns revealed the formation of three polymorphs over time: α, β' and β. As illustrated in Fig. 3b, the appearance of a WAXD peak with apparent maxima at ~0.412 nm was attributed to the formation of the α polymorph; peaks with apparent maxima at 0.422–0.435 nm and ~0.38 nm were attributed to the β' polymorph; and a peak at ~0.46 nm was assigned to the β polymorph. The α peak appeared simultaneously with a SAXD peak corresponding to a lamellar thickness of 4.5–4.7 nm, whereas the β' and β peaks were recorded simultaneously with a single SAXD peak corresponding to a lamellar thickness of 4.0–4.3 nm. The occurrence of a single SAXD peak for coexisting β' and β phases is typical for MF (Arita-Merino et al., 2022). All lamellar thicknesses were within the range of the length of two acyl chains, which indicated that the crystals had a double chain configuration (2L). Therefore, the phases corresponded to α-2, β'-2 and β-2 structures. For simplicity, we refer to them herein as α, β' and β.

The differences in the diffraction peaks showed variations in the levels of the polymorphs formed in the four samples (Fig. 3b). To quantify these differences, we performed quantitative phase analysis using the time-resolved WAXD patterns as described in Section 2.5.1 and in further detail elsewhere (Arita-Merino et al., 2020). From this analysis, we obtained phase transition diagrams in which the mass fraction of the different polymorphs was plotted over time (Fig. 3c). The maximum levels of each polymorph are included in Table 3.

In line with the isothermal DSC results (Fig. 2c), the CON with *DGAT1* AA sample showed a 1-step crystallization process involving the formation of β' and β polymorphs from the melt, while the other three samples displayed 2-step crystallization processes corresponding to the initial formation of α and, subsequently, β' and β polymorphs. The amount of α polymorph declined while the levels of β' polymorph increased, indicating a polymorphic transition from α to β'. The formation of a β' polymorph, mediated by the initial formation of an α polymorph, is common in MF (Arita-Merino et al., 2022; Tzompa-Sosa et al., 2016; Wiking et al., 2009). The transition and abundance of the phases could be explained by the compositional differences.

As the phase transition diagrams in Fig. 3c show, β' was the most abundant (10–17 %) polymorph in all the samples, which is typical for MF at 20 °C (Arita-Merino et al., 2022; Tzompa-Sosa & Arita-Merino, 2022). However, the amount of β' polymorph was lower for the LSO supplementation samples compared to the CON samples, and this effect was more pronounced for the *DGAT1* AA pair (6 % lower) than for the *DGAT1* KK pair (3 % lower). Although the *DGAT1* KK samples consistently showed higher β' polymorph levels than the *DGAT1* AA samples, the difference was sizeable only for the LSO supplementation pair (4 % higher). The levels of β' polymorph aligned with the TG profiles (Table 2); the reduction in the majority of the saturated TGs after LSO supplementation corresponded with the clear reductions in β' polymorph. Moreover, the pronounced difference between the LSO supplementation samples with different *DGAT1* could be explained by the synergistic increase in unsaturated HMW TGs for the combination of LSO and *DGAT1* AA (Table 2).

The differences for the other polymorphs were not as clear as for β', as only small amounts of α (0–2 %) and β (1–2 %) polymorphs were formed. The formation of the α polymorph was higher for the *DGAT1* KK samples (2 %) than for the *DGAT1* AA samples (0 % with CON and 1 % with LSO supplementation), but we observed no difference in relation to diet. This coincided with the lack of a clear diet effect on the melting endset (by DSC), as well as the higher melting endset values for the *DGAT1* KK samples (Table 3). Additionally, we did not find α polymorph formation in the CON with *DGAT1* AA sample, which matched the distinctively lower crystallization onset and T_{HCT} (by DSC) of that sample (Table 3). Thus, we suggest that two similar groups of TGs contribute to the formation of the α polymorph at 20 °C. The first has the highest crystallization temperature and thus defines the crystallization onset and affects the T_{HCT}; these TGs are present in a lower concentration in the CON with *DGAT1* AA sample but are likely to be in comparable levels in the other three samples. The second TG group melts at the highest temperature and thus determines the melting endset; these TGs are higher in the *DGAT1* KK samples. As mentioned previously, the TGs in this group are not necessarily the largest saturated molecules, as the MF melting profile is not only determined by the melting point of individual TGs but also by their inter-miscibility. According to the TG profile of the *DGAT1* KK, we suggest that a group of odd-chain saturated TGs is responsible for the increase in melting endset and α polymorph formation associated with this *DGAT1* variant. However, we could not identify a specific group of HCT TGs that were distinctively low in the CON with *DGAT1* AA sample to associate with the formation of the α polymorph, the crystallization onset and the T_{HCT}.

For the β polymorph, the same levels (1 %) were formed in all samples except for the LSO supplementation with *DGAT1* KK sample, in which there was a higher amount of the polymorph (2 %). In previous studies (Arita-Merino et al., 2022; Tzompa-Sosa et al., 2016), we concluded that a specific group of β-tending TGs was responsible for the limited formation of β polymorph in MF. High levels of unsaturated TGs corresponding to groups C52–C54 have been related to the occurrence of β polymorph in MF (Tzompa-Sosa et al., 2016). Accordingly, we expected an association between LSO supplementation and β polymorph, but this was not the case; while the levels of C52–C54 in both CON samples and the LSO supplementation with *DGAT1* AA sample varied considerably (13–28 g/100 g; Table 1), the same amount (1 %) of β

polymorph was formed in these three samples. In contrast, a higher β polymorph formation (2 %) was observed for the LSO supplementation with *DGAT1* KK sample, even though it contained 4 g/100 g less CN52–C54 than the LSO supplementation with *DGAT1* AA sample (Table 1), as well as a lower proportion of unsaturated HMW TGs (Table 2). Thus, we could not confirm the link between unsaturated HMW TGs and the β polymorph. Given the limited number of samples (n = 4), our results do not clarify which specific TG species form the β polymorph.

Regardless of the subcell structure, the SAXD patterns (Fig. 3a) showed signs of differences in lamellar thickness between the samples. We used SAXS to evaluate these differences in detail and determine whether an effect was observable on the next structural level. As shown in Fig. 3d, we precisely determined the center and the full width at half maximum (FWHM) of the first-order SAXS peak recorded after 1 h at 20 °C. These values were used to calculate the lamellar thickness and the average crystallite size (ACS) (Table 3), respectively. The ACS obtained from SAXS patterns corresponded to the nanoplatelet thickness (Acevedo & Marangoni, 2010), which was determined by the thickness and number of lamellae building the nanoplatelets.

Diet was clearly related to changes in lamellar thickness; the LSO supplementation samples displayed thicker lamellae than the CON samples (0.15–0.16 nm thicker). As lamellae are layers of stacked TGs, their thickness is largely determined by the chain length of the FAs. Therefore, the increase in C_{18} FAs with LSO supplementation (van Gastelen et al., 2017) explained the differences in lamellar thickness (Table 3). These results aligned with the findings of Bugeat et al. (2015) regarding UFA-enriched MF; although they did not study isothermal crystallization, they reported an increase in lamellar thickness in the crystalline phases observed during cooling and heating, and attributed this increase to the incorporation of long-chain FAs into the crystals. Additionally, in our study, the *DGAT1* KK samples consistently displayed thinner lamellae than the *DGAT1* AA samples (0.01–0.02 nm thinner), which may have been due to a decrease in some unsaturated C_{18} FAs associated with *DGAT1* KK (van Gastelen et al., 2017). Nevertheless, a higher number of observations is required to confirm this minor effect.

Despite the differences in lamellar thickness, the two CON samples and the sample for LSO supplementation with *DGAT1* KK had comparable ACS (56–57 nm), but the sample for LSO supplementation with *DGAT1* AA had a lower value (52 nm). Studies in other lipid systems have shown that nanoplatelet thickness decreases with higher driving forces for crystallization (Acevedo & Marangoni, 2010; Nikolaeva et al., 2018). However, the sample for LSO supplementation with *DGAT1* AA had the lowest β' polymorph formation (Table 3), which implied that it had the lowest driving force for crystallization. To the extent of our knowledge, no other studies have examined the effect of compositional changes on the nanoplatelet thickness of MF, and thus, more research is needed in this regard to link crystallite size to TG composition.

3.3. Technological relevance

From a technological perspective, our findings could be of value for regulating MF properties. For example, LSO supplementation could improve the nutritional profile of dairy products, increasing the levels of unsaturated TGs in the human diet. Our results showed that higher levels of polyunsaturated TGs (i.e. TG 54:4, TG 54:3 and TG 54:2) could be obtained from cows with *DGAT1* AA and LSO supplementation. This indicates possible routes for regulating the functional and sensory properties of products containing high levels of MF. Consumers have experienced increased butter hardness and melting temperature (Marangoni et al., 2022), characteristics that are also observed in winter in countries where MF displays seasonal variation (Staniewski et al., 2021). LSO supplementation could be used to control the levels of β' polymorph, the main contributor to the SFC in MF, thereby helping to regulate the hardness of butter and cheese. The selection of cows with *DGAT1* AA could also help to reduce the melting temperature of butter, as we found an association between *DGAT1* KK, HMF and the melting endset of MF. Conversely, the production of MF with a higher proportion of HMF by cows with *DGAT1* KK could be favorable for producing MF stearin, a valuable ingredient for bakery and confectionery applications (Gibon, 2006).

Whether LSO supplementation is implemented to control SFC levels in MF, to improve MF nutritional value, or reduce methane emissions from milk production (van Gastelen et al., 2017), the possible negative effects on MF functionality need to be evaluated. The increase in unsaturated HMW TGs with LSO supplementation, as well as enhancement with *DGAT1* AA, could have led to an increased formation of β polymorph (Tzompa-Sosa et al., 2016). However, we showed that the increase in unsaturated HMW TGs was not related to the levels of β polymorph in MF, which could have been a drawback, as the formation of β polymorph is commonly associated with an undesirable grainy texture and low spreadability (Sato & Ueno, 2011).

4. Conclusions

This study showed that the cow's genetics had specific effects on TG composition and, consequently, on MF crystallization. An unsaturated diet (LSO supplementation) increased the levels of unsaturated TGs (C40 and C52). The higher proportion of unsaturated TGs was linked to changes in MF crystallization and melting, most notably, with an additional crystallization peak, an increased proportion of low-melting fraction, a reduction in β' polymorph and the formation of thicker lamellae. Variant KK of the *DGAT1*, was associated with higher levels of odd-chain saturated TG 31:0–TG 41:0 and monounsaturated TG 37:1 and TG 41:1. This change in TAG profile was associated with increments in the melting endset and the formation of α polymorph, parameters that appeared to be unaffected by diet. Although we observed differences in the formation of β polymorph and the nanoplatelet thickness, we could not identify trends in relation to diet nor *DGAT1*. This work confirms and extends the knowledge on MF crystallization as affected by its TG profile and, for the first time, provides information on the effect of *DGAT1* on MF crystallization.

The design of this experimental study allowed us to draw conclusions specific to LSO supplementation, *DGAT1* polymorphism and their interaction. Other factors known to affect MF composition (e.g. stage of lactation and breed) might influence the responses we reported, future studies could focus on evaluating those interactions prior to the implementation of LSO supplementation or selective breeding. We also recommend further research to identify the role of different TG groups in other aspects of MF crystallization, such as nanoplatelet thickness and the formation of β polymorphs.

CRediT authorship contribution statement

N. Arita-Merino: Conceptualization, Data curation, Formal analysis, Funding acquisition, Investigation, Methodology, Writing – original draft, Writing – review & editing. **S. Yener:** Conceptualization, Data curation, Formal analysis, Methodology, Supervision, Writing – original draft, Writing – review & editing. **H.J.F. van Valenberg:** Conceptualization, Funding acquisition, Project administration, Resources, Supervision, Writing – review & editing. **J. Dijkstra:** Conceptualization, Funding acquisition, Investigation, Methodology, Project administration, Resources, Supervision, Validation, Writing – review & editing. **S. van Gastelen:** Conceptualization, Funding acquisition, Investigation, Methodology, Project administration, Resources, Validation, Writing – review & editing. **E. Scholten:** Conceptualization, Investigation, Methodology, Project administration, Supervision, Writing – review & editing. **D.A. Tzompa-Sosa:** Conceptualization, Data curation, Formal analysis, Investigation, Methodology, Writing – original draft, Writing – review & editing.

Declaration of Competing Interest

The authors declare that they have no known competing financial interests or personal relationships that could have appeared to influence the work reported in this paper.

Data availability

Data will be made available on request.

Acknowledgements

This work was supported by CONACYT, the National Council of Science and Technology of Mexico (grant number 474601). We thank FWO from the Belgian government for the grant given to acquire the SAXS equipment (grant AUGE/17/29). Milk samples were obtained from an experiment conducted by Wageningen University and Research as part of the TI Food and Nutrition program "Reduced methane emissions from dairy cows: Towards sustainable dairy cattle production by increased understanding of genetic variation and rumen functioning."

References

Acevedo, N. C., & Marangoni, A. G. (2010). Toward nanoscale engineering of triacylglycerol crystal networks. *Crystal Growth & Design, 10*(8), 3334–3339. https://doi.org/10.1021/cg100469x

Acevedo, N. C., & Marangoni, A. G. (2015). Nanostructured fat crystal systems. *Annual Review of Food Science and Technology, 6*(1), 71–96. https://doi.org/10.1146/annurev-food-030713-092400

Arita-Merino, N., te Nijenhuis, L., van Valenberg, H., & Scholten, E. (2022). Multiple phase transitions and microstructural rearrangements shape milk fat crystal networks. *Journal of Colloid and Interface Science, 607*, 1050–1060. https://doi.org/10.1016/j.jcis.2021.09.071

Arita-Merino, N., van Valenberg, H., Gilbert, E. P., & Scholten, E. (2020). Quantitative phase analysis of complex fats during crystallization. *Crystal Growth & Design, 20*(8), 5193–5202. https://doi.org/10.1021/acs.cgd.0c00416

Bocquel, D., Marquis, R., Dromard, M., Salamin, P.-A., Rey-Siggen, J., Héritier, J., … Andlauer, W. (2016). Effect of flaxseed supplementation of dairy cows' forage on physicochemical characteristic of milk and Raclette cheese. *International Journal of Dairy Technology, 69*(1), 129–136. https://doi.org/10.1111/1471-0307.12235

Bugeat, S., Perez, J., Briard-Bion, V., Pradel, P., Ferlay, A., Bourgaux, C., & Lopez, C. (2015). Unsaturated fatty acid enriched vs. control milk triacylglycerols: Solid and liquid TAG phases examined by synchrotron radiation X-ray diffraction coupled with DSC. *Food Research International, 67*, 91–101. https://doi.org/10.1016/j.foodres.2014.10.029

Castro, T., Martinez, D., Isabel, B., Cabezas, A., & Jimeno, V. (2019). Vegetable oils rich in polyunsaturated fatty acids supplementation of dairy cows' diets: Effects on productive and reproductive performance. *Animals, 9*(5). https://doi.org/10.3390/ani9050205

DePeters, E. J., German, J. B., Taylor, S. J., Essex, S. T., & Perez-Monti, H. (2001). Fatty acid and triglyceride composition of milk fat from lactating Holstein cows in response to supplemental canola oil. *Journal of Dairy Science, 84*(4), 929–936. https://doi.org/10.3168/jds.S0022-0302(01)74550-X

Fahy, E., Sud, M., Cotter, D., & Subramaniam, S. (2007). LIPID MAPS online tools for lipid research. *Nucleic Acids Research, 35*(Web Server), W606–W612. 10.1093/nar/gkm324.

Fuchs, B., Süß, R., & Schiller, J. (2010). An update of MALDI-TOF mass spectrometry in lipid research. *Progress in Lipid Research, 49*(4), 450–475. https://doi.org/10.1016/j.plipres.2010.07.001

Gibon, V. (2006). Fractionation of lipids for use in food. In *Modifying Lipids for Use in Food* (pp. 201–233). Elsevier. https://doi.org/10.1533/9781845691684.2.201.

Gresti, J., Bugaut, M., Maniongui, C., & Bezard, J. (1993). Composition of molecular species of triacylglycerols in bovine milk fat. *Journal of Dairy Science, 76*(7), 1850–1869. https://doi.org/10.3168/jds.S0022-0302(93)77518-9

Guyon, F., Absalon, C., Eloy, A., Salagoity, M. H., Esclapez, M., & Medina, B. (2003). Comparative study of matrix-assisted laser desorption/ionization and gas chromatography for quantitative determination of cocoa butter and cocoa butter equivalent triacylglycerol composition. *Rapid Communications in Mass Spectrometry, 17*(20), 2317–2322. https://doi.org/10.1002/rcm.1185

IDF-ISO. (2010). *17678-IDF 202 16958-IDF 231. Milk and milk products - Determination of milk fat purity by gas chromatographic analysis of triglycerides (Reference method)*. International Dairy Federation.

ISO-IDF. (2004). *ISO 14637:2004 | IDF 195:2004 Milk — Determination of urea content — Enzymatic method using difference in pH (Reference method)*.

Jacobs, A. A. A., van Baal, J., Smits, M. A., Taweel, H. Z. H., Hendriks, W. H., van Vuuren, A. M., & Dijkstra, J. (2011). Effects of feeding rapeseed oil, soybean oil, or linseed oil on stearoyl-CoA desaturase expression in the mammary gland of dairy cows. *Journal of Dairy Science, 94*(2), 874–887. https://doi.org/10.3168/jds.2010-3511

Kaupe, B., Winter, A., Fries, R., & Erhardt, G. (2004). DGAT1 polymorphism in Bos indicus and Bos taurus cattle breeds. *Journal of Dairy Research, 71*(2), 182–187. https://doi.org/10.1017/S0022029904000032

Liu, Z., Li, C., Pryce, J., & Rochfort, S. (2020). Comprehensive characterization of bovine milk lipids: Triglycerides. *ACS Omega, 5*(21), 12573–12582. https://doi.org/10.1021/acsomega.0c01841

Lopez, C. (2018). Crystallization properties of milk fats. In K. Sato (Ed.), *Crystallization of lipids* (pp. 283–321). Ltd: John Wiley & Sons. https://doi.org/10.1002/9781118593882.ch10.

Lopez, C., Lesieur, P., Bourgaux, C., & Ollivon, M. (2005). Thermal and structural behavior of anhydrous milk fat. 3. Influence of cooling rate. *Journal of Dairy Science, 88*(2), 511–526. https://doi.org/10.3168/jds.S0022-0302(05)72713-2

Lu, J., Boeren, S., van Hooijdonk, T., Vervoort, J., & Hettinga, K. (2015). Effect of the DGAT1 K232A genotype of dairy cows on the milk metabolome and proteome. *Journal of Dairy Science, 98*(5), 3460–3469. https://doi.org/10.3168/jds.2014-8872

Marangoni, A. G., Ghazani, S. M., Gammage, S., Van Rosendaal, J., Music, J., & Charlebois, S. (2022). Higher palmitic acid and dipalmitoyloleate levels are correlated to increased firmness in commercial butter. *Food Chemistry*, *377*(August 2021), 131991. 10.1016/j.foodchem.2021.131991.

Näslund, J., Fikse, W. F., Pielberg, G. R., & Lundén, A. (2008). Frequency and effect of the bovine Acyl-CoA: Diacylglycerol acyltransferase 1 (DGAT1) K232A polymorphism in Swedish dairy cattle. *Journal of Dairy Science, 91*(5), 2127–2134. https://doi.org/10.3168/jds.2007-0330

Nikolaeva, T., Adel, R. D., Velichko, E., Bouwman, W. G., Hermida-Merino, D., Van As, H., … Van Duynhoven, J. (2018). Networks of micronized fat crystals grown under static conditions. *Food and Function, 9*(4), 2102–2111. https://doi.org/10.1039/c8fo00148k

Pacheco-Pappenheim, S., Yener, S., Heck, J. M. L., Dijkstra, J., & van Valenberg, H. J. F. (2021). Seasonal variation in fatty acid and triacylglycerol composition of bovine milk fat. *Journal of Dairy Science, 104*(8), 8479–8492. https://doi.org/10.3168/jds.2020-19856

Pacheco-Pappenheim, S., Yener, S., Nichols, K., Dijkstra, J., Hettinga, K., & van Valenberg, H. J. F. (2022). Feeding hydrogenated palm fatty acids and rumen-protected protein to lactating Holstein-Friesian dairy cows modifies milk fat triacylglycerol composition and structure, and solid fat content. *Journal of Dairy Science*. https://doi.org/10.3168/jds.2021-21083

Pacheco-Pappenheim, S., Yener, S., van Valenberg, H. J. F., Tzompa-Sosa, D. A., & Bovenhuis, H. (2019). The DGAT1 K232A polymorphism and feeding modify milk fat triacylglycerol composition. *Journal of Dairy Science, 102*(8), 6842–6852. https://doi.org/10.3168/jds.2019-16554

Palmquist, D. L. (2006). Milk fat: Origin of fatty acids and influence of nutritional factors thereon. In P. F. Fox & P. L. H. McSweeney (Eds.), *Advanced Dairy Chemistry Volume 2 Lipids* (3rd ed., Vol. 2, pp. 43–92). Springer. 10.1007/0-387-28813-9_2.

Picariello, G., Sacchi, R., & Addeo, F. (2007). One-step characterization of triacylglycerols from animal fat by MALDI-TOF MS. *European Journal of Lipid Science and Technology, 109*(5), 511–524. https://doi.org/10.1002/ejlt.200600255

Sato, K., & Ueno, S. (2011). Crystallization, transformation and microstructures of polymorphic fats in colloidal dispersion states. *Current Opinion in Colloid & Interface Science, 16*(5), 384–390. https://doi.org/10.1016/j.cocis.2011.06.004

Schennink, A., Heck, J. M. L., Bovenhuis, H., Visker, M. H. P. W., Van Valenberg, H. J. F., & Van Arendonk, J. A. M. (2008). Milk fatty acid unsaturation: Genetic parameters and effects of stearoyl-CoA desaturase (SCD1) and Acyl CoA: Diacylglycerol acyltransferase 1 (DGAT1). *Journal of Dairy Science, 91*(5), 2135–2143. https://doi.org/10.3168/jds.2007-0825

Smet, K., Coudijzer, K., Fredrick, E., De Campeneere, S., De Block, J., Wouters, J., … Dewettinck, K. (2010). Crystallization behavior of milk fat obtained from linseed-fed cows. *Journal of Dairy Science, 93*(2), 495–505. https://doi.org/10.3168/jds.2009-2588

Soyeurt, H., Gillon, A., Vanderick, S., Mayeres, P., Bertozzi, C., & Gengler, N. (2007). Estimation of heritability and genetic correlations for the major fatty acids in bovine milk. *Journal of Dairy Science, 90*(9), 4435–4442. https://doi.org/10.3168/jds.2007-0054

Staniewski, B., Ogrodowska, D., Staniewska, K., & Kowalik, J. (2021). The effect of triacylglycerol and fatty acid composition on the rheological properties of butter. *International Dairy Journal, 114*, Article 104913. https://doi.org/10.1016/j.idairyj.2020.104913

Tzompa-Sosa, D. A., van Aken, G. A., van Hooijdonk, A. C. M., & van Valenberg, H. J. F. (2014). Influence of C16:0 and long-chain saturated fatty acids on normal variation of bovine milk fat triacylglycerol structure. *Journal of Dairy Science, 97*(7), 4542–4551. https://doi.org/10.3168/jds.2014-7937

Tzompa-Sosa, D. A., van Valenberg, H. J. F., van Aken, G. A., & Bovenhuis, H. (2016). Milk fat triacylglycerols and their relations with milk fatty acid composition, DGAT1 K232A polymorphism, and milk production traits. *Journal of Dairy Science, 99*(5), 3624–3631. https://doi.org/10.3168/jds.2015-10592

Tzompa-Sosa, D.A., & Arita-Merino, N. (2022). Advances in dairy lipid science: physicochemical aspects. In T. Huppertz & T. Vasiljevic (Eds.), *Understanding and improving the functional and nutritional properties of milk* (1st ed., pp. 305–340). Burleigh Dodds Science Publishing. 10.19103/AS.2022.0099.08.

Tzompa-Sosa, D. A., Ramel, P. R., van Valenberg, H. J. F., & van Aken, G. A. (2016). Formation of β polymorphs in milk fats with large differences in triacylglycerol profiles. *Journal of Agricultural and Food Chemistry, 64*(20), 4152–4157. https://doi.org/10.1021/acs.jafc.5b05737

Tzompa-Sosa, D. A., Meurs, P. P., & van Valenberg, H. J. F. (2018). Triacylglycerol profile of summer and winter bovine milk fat and the feasibility of triacylglycerol fragmentation. *European Journal of Lipid Science and Technology, 120*(3), 1700291. https://doi.org/10.1002/ejlt.201700291

van Gastelen, S., Visker, M. H. P. W., Edwards, J. E., Antunes-Fernandes, E. C., Hettinga, K. A., Alferink, S. J. J., … Dijkstra, J. (2017). Linseed oil and DGAT1 K232A polymorphism: Effects on methane emission, energy and nitrogen metabolism, lactation performance, ruminal fermentation, and rumen microbial composition of Holstein-Friesian cows. *Journal of Dairy Science, 100*(11), 8939–8957. https://doi.org/10.3168/jds.2016-12367

Vanbergue, E., Hurtaud, C., Peyraud, J.-L., Beuvier, E., Duboz, G., & Buchin, S. (2018). Effects of n-3 fatty acid sources on butter and hard cooked cheese; technological properties and sensory quality. *International Dairy Journal, 82*, 35–44. https://doi.org/10.1016/j.idairyj.2018.03.002

Wiking, L., de Graef, V., Rasmussen, M., & Dewettinck, K. (2009). Relations between crystallisation mechanisms and microstructure of milk fat. *International Dairy Journal, 19*(8), 424–430. https://doi.org/10.1016/j.idairyj.2009.03.003

Wright, A. J., Hartel, R. W., Narine, S. S., & Marangoni, A. G. (2000). The effect of minor components on milk fat crystallization. *Journal of the American Oil Chemists' Society, 77*(5), 463–475. https://doi.org/10.1007/s11746-000-0075-8

Wright, A. J., & Marangoni, A. G. (2003). The effect of minor components on milk fat microstructure and mechanical properties. *Journal of Food Science, 68*, 182–186. https://doi.org/10.1111/j.1365-2621.2003.tb14137.x

Wright, A. J., McGauley, S. E., Narine, S. S., Willis, W. M., Lencki, R. W., & Marangoni, A. G. (2000). Solvent effects on the crystallization behavior of milk fat fractions. *Journal of Agricultural and Food Chemistry, 48*(4), 1033–1040. https://doi.org/10.1021/jf9908244